HHS Public Access

Author manuscript

Chem Res Toxicol. Author manuscript; available in PMC 2017 November 21.

Published in final edited form as:

Chem Res Toxicol. 2016 November 21; 29(11): 1894–1900. doi:10.1021/acs.chemrestox.6b00318.

DNA Polymerase ν Rapidly Bypasses O^6-Methyl-dG but Not O^6-[4-(3-Pyridyl)-4-oxobutyl-dG and O^2-Alkyl-dTs

A. S. Prakasha Gowda and **Thomas E. Spratt***

Department of Biochemistry and Molecular Biology, Penn State College of Medicine, Pennsylvania State University, Hershey, Pennsylvania 17033, United States

Abstract

4-(Methylnitrosamino)-1-(3-pyridyl)-1-butanone (NNK) is a potent tobacco carcinogen that forms mutagenic DNA adducts including O^6-methyl-2′-deoxyguanosine (O^6-Me-dG), O^6-[4-(3-pyridyl)-4-oxobut-1-yl]-dG (O^6-POB-dG), O^2-methylthymidine (O^2-Me-dT), and O^2-POB-dT. We evaluated the ability of human DNA polymerase ν to bypass this damage to evaluate the structural constraints on substrates for pol ν and to evaluate if there is kinetic evidence suggesting the in vivo activity of pol ν on tobacco-induced DNA damage. Presteady-state kinetic analysis has indicated that O^6-Me-dG is a good substrate for pol ν, while O^6-POB-dG and the O^2-alkyl-dT adducts are poor substrates for pol ν. The reactivity with O^6-Me-dG is high with a preference for dCTP > dGTP > dATP > dTTP. The catalytic activity of pol ν toward O^6-Me-dG is high and can potentially be involved in its bypass in vivo. In contrast, pol ν is unlikely to bypass O^6-POB-dG or the O^2-alkyl-dTs in vivo.

Graphical Abstract

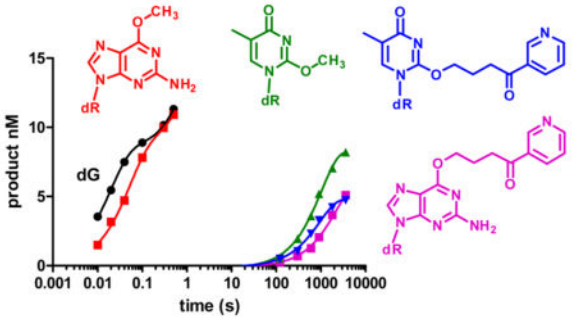

*Corresponding Author: Tel: 717-531-4623. tes13@psu.edu.

Notes

The Pennsylvania Department of Health specifically disclaims responsibility for any analyses, interpretations or conclusions. The authors declare no competing financial interest.

Supporting Information

The Supporting Information is available free of charge on the ACS Publications website at DOI: 10.1021/acs.chemres-tox.6b00318.

Steady-state and polymerase in excess analyses and results from computer simulations (PDF)

Script and data used to perform the computer simulations (ZIP)

INTRODUCTION

Tobacco and its smoke contains over 4000 compounds and 70 carcinogens.[1–4] 4-(Methylnitrosamino)-1-(3-pyridyl)-1-buta-none (NNK), one of the more potent carcinogens in tobacco, produces both methyl (Me) and 4-(3-pyridyl)-4-oxobutyl (POB) DNA adducts. Both of these classes of DNA adducts play a role in carcinogenesis.[5,6] In particular, O^6-Me-dG, O^6-POB-dG, and O^2-POB-dT (Chart 1) have been implicated in the mutagenicity of NNK.[7–9]

The potent mutagenicity of O^6-Me-dG is long known. In vitro studies have shown that many polymerases insert dTTP opposite O^6-Me-dG.[10,11] When compared with dG in the template, the k_{cat}/K_m values for the incorporation of dCTP opposite O^6-Me-dG decrease 2–3 orders of magnitude, while that for dTTP increase 1 to 2 orders of magnitude for a variety of polymerases including the Klenow fragment of *E. coli* DNA polymerase I (Kf) *Thermus aquaticus* pol I, HIV reverse transcriptase, T7 pol, pol δ/PCNA, pol η, pol κ, and pol ι.[10,12–16] Loveless proposed that dTTP is incorporated opposite O^6-Me-dG because it is able to form a Watson–Crick-like structure as illustrated in Figure 1A.[17] In contrast, dC forms a wobble base pair with O^6-Me-dG (Figure 1B). The exact nature of the base pair in the polymerase active site has been elusive. While a function/kinetic study supported a Watson–Crick-like base pair between dT and O^6-Me-dG,[16] a crystallization study with *Bacillus stearothermophilus* DNA polymerase I large fragment (BF) found the dT/O^6-Me-dG base pair to be that in Figure 1C, while the dC/O^6-Me-dG base pair was Watson–Crick like as shown in Figure 1D.[18] The question of which polymerase(s) bypass this adduct in vivo still remains. While pol η is the most active eukaryotic Y-family polymerase with O^6-Me-dG, the replicative polymerase pol δ is also quite active.[19]

O^6-POB-dG is mutagenic in HEK293 cells, causing primarily G to A mutations, consistent with dT pairing with O^6-POB-dG.[8] In vitro studies have shown that O^6-POB-dG is a poorer substrate than O^6-Me-dG for pol η, κ, and ι.[13] Similar to O^6-Me-dG, pol η has the highest reactivity for O^6-POB-dG.[13]

O^2-POB-dT may also play a role in NNK mutagenesis, as it is the most abundant POB-adduct in rodents. Bypass of O^2-alkyl-dTs requires TLS polymerases in *E. coli*[20,21] as well as human cells.[9] In human cells, the bypass of O^2-Me-dT and O^2-POB-dT requires pol η, ζ, and Rev1.[9] In vitro kinetics studies show that pol η is the most active Y-family polymerase in the bypass of O^2-alkyl-dTs[22–25] However, the activity is low, and there remains a possibility that another polymerase is involved in the bypass of O^2-alkyl-dTs.

DNA polymerase ν is an A-family polymerase, with a mutation rate similar to Y-family polymerases.[26] The polymer-ase is especially unfaithful with a high propensity for the formation of dG/dT mismatches.[26,27] The polymerase has been implicated in the bypass of interstrand cross-links and can also bypass damage in the major groove of the DNA.[28,29] Since the dT/dG mispair forms structures similar to the dC/O^6-Me-dG and dT/O^2-Me-dT base pairs,[18,30,31] we hypothesized that pol ν can bypass O^6-Me-dG. The ability of pol ν to bypass bulky major groove adducts led us to hypothesize that pol ν can bypass the bulky O^6-POB-dG. Because O^2-Me-dT can potentially form a wobble or Watson–Crick structures

with dA or dG, we also evaluated the reactivity of pol ν with O^2-Me-dT and the tobacco-relevant O^2-POB-dT.

EXPERIMENTAL SECTION

General

[γ-^{32}P]ATP was purchased from PerkinElmer and T4 polynucleotide kinase from USB/Aflymetrix. The dNTPs (ultrapure grade) were purchased from GE Healthcare, and the concentrations were determined by UV absorbance.[32] Oligodeoxynucleotides were synthesized at the Macromolecular Core facility at the PSU College of Medicine. The phosphoramidite for O^6-Me-dG was purchased from Glen Research (Sterling, VA). The oligodeoxynucleotides containing O^6-POB-dG, O^2-Me-dT, and O^2-POB-dT were synthesized as described.[24,25,33,34] The sequences of the oligodeoxynucleotides are shown in Chart 2 in which X was dG, O^6-Me-dG, O^6-POB-dG, and Y was dT, O^2-Me-dT, and O^2-POB-dT. The primer was ^{32}P-labeled with [γ-^{32}P]ATP and annealed with a 20% excess of the template as previously described.[35]

Pol ν was purified by a modification of the method of Takata et al.[26] as we previously described.[35] The protein has a deletion of a C-terminal poly proline segment, an N-terminal His-tag, and C-terminal FLAG-tag. After lysing the cells, the resulting supernatant was loaded onto a Ni-NTA column (3 mL) and the enzyme eluted with an imidazole gradient. Purity was evaluated by SDS–PAGE and the protein concentration determined by the Qubit protein assay kit (Life Technologies). The active concentration was determined by performing burst kinetics with an excess of DNA.[35]

Kinetic Analyses

All reactions were performed in 40 mM Tris-HCl (pH 8.0) and 5 mM $MgCl_2$ at 37 °C. The concentrations reported for each species are those that occurred during the reaction. The reactions were initiated by the addition of dNTP containing $MgCl_2$ to preincubated protein and DNA in buffer. Steady-state reactions were performed with 0.1 to 1 nM polymerase and 20–30 nM DNA. The enzyme in excess reactions were conducted with 150 nM polymerase and 15 nM DNA. Slow reactions were quenched with equal volumes of STOP solution containing 10% 0.5 M Na_2EDTA, 90% formamide, and 0.025% (w/v) xylene cyanol and bromophenol blue. Fast reactions were carried out with an RQF-3 quench flow apparatus (Kin Tek) and were quenched with 0.3 M Na_2EDTA, which was diluted with STOP solution to load on the gel. The progress of the reaction was analyzed by denaturing PAGE, and the radioactivity on the gel was visualized with a Typhoon 9200. The reactions were quantitated by dividing the total radioactivity in the product band(s) by the radioactivity in the product and reactant bands.

Data Analysis

The kinetic constants were fit using GraphPad Prism V5. Computer simulations were performed with DynaFit Version 4 (BioKin Ltd.).[36] The steady-state initial rate reactions were fit to the Michelis–Menten equation in eq 1. The time course experiments were fit to the burst equation (eq 2), in which P is the concentration of the product at various times (t),

A the amplitude, and k and k_{ss} are the rapid and steady-state rate constants. If the burst rate constant demonstrated a dNTP dependence, it was fit to eq 3 in which k was the burst rate constant and K_d^{dNTP} the apparent dNTP dissociation constant. Similarly, if the burst amplitude exhibited a dNTP concentration dependence, it was fit to the hyperbolic equation to obtain A_{max} and K_A values.

$$v=\frac{V_{\max}[\mathrm{dNTP}]}{[\mathrm{dNTP}]+K_m} \quad (1)$$

$$P=A(1-\mathrm{e}^{-kt})+k_{ss}t \quad (2)$$

$$k=\frac{k_{\mathrm{pol}}[\mathrm{dNTP}]}{[\mathrm{dNTP}]+K_d^{\mathrm{dNTP}}} \quad (3)$$

RESULTS

To gain more information about the activity of pol ν, we examined the incorporation of dNTPs opposite four DNA adducts, O^6-Me-dG, O^6-POB-dG, O^2-Me-dT, and O^2-POB-dT. The steady state rate constants were determined, and the results are presented in Table 1. The k_{cat}/K_m values are summarized in Figure 2. dCTP was inserted opposite dG with a k_{cat}/K_m value of 5220 M^{-1} s^{-1}. The fidelity with undamaged DNA is poor, as expected.[27,37] dTTP, is incorporated with a k_{cat}/K_m of 264 M^{-1} s^{-1}, which corresponds to an f_{inc} = 0.05. Discrimination against dATP and dGTP were only slightly better, with f_{inc} values of 0.011 and 0.014, respectively.

With O^6-Me-dG as the template base, the k_{cat}/K_m for dCTP decreased 316-fold, while the k_{cat}/K_m for dTTP incorporation decreased 49-fold. This effect differs from that observed with Kf(exo-) and Taq polymerase, two high fidelity A-family polymerases. Several studies have shown that the k_{cat}/K_m for dCTP incorporation decreases 10,000-fold, while that for dTTP incorporation increases ~100-fold, thereby giving a preference for dTTP incorporation opposite O^6-Me-dG.[10,16] In contrast to other polymerases, methylation of the O^6-position did not increase the k_{cat}/K_m of dTTP, and pol ν retains its preference for dCTP incorporation. In addition, the k_{cat}/K_m values for the incorporation of dG and dA were very similar to that of dT. Thus, pol ν does not have any preference to insert dTTP opposite O^6-Me-dG. We observed a similar pattern with the larger O^6-POB-dG, with k_{cat}/K_m values that are 2–5-fold lower than those for O^6-Me-dG.

With dT as the template base, while the k_{cat}/K_m for correct incorporation was less than that for dG as template, but the fidelity was similar. We found the k_{cat}/K_m for the incorporation of dGTP opposite dC to be 13-fold greater than the incorporation of dATP opposite dT. Methylation of the O^2-position decreases k_{cat}/K_m for dATP incorporation 160-fold, a value

that is similar to the effect caused by the dG to O^6-Me-dG. The O^2-methylation, however, essentially abolishes the specificity of the incorporation. The k_{cat}/K_m values for dNTP incorporation are all within a factor of 3. Pyridyloxobutylation of the O^2-position further reduces the k_{cat}/K_m 2–4-fold and similarly abolishes specificity.

The in vitro activities of DNA polymerases are limited by the rate limiting dissociation of the DNA from the polymerase. With respect to pol ν, the reactivity is also limited by a rate limiting conformational change after phosphodiester bond formation. Thus, Michaelis–Menten kinetics may not reflect the phosphoryl-transfer activity of the polymerase. Therefore, we examined the reaction with DNA polymerase in excess over the DNA to examine the rate of phosphodiester bond formation.

Figure 3 shows the plots with 150 nM pol ν, 15 nM DNA, and 50 μM dNTP. At this concentration of DNA and polymerase, 95% of the DNA should be bound to polymerase, assuming that the modification does not alter the K_d of the pol to undamaged DNA.[35] dCTP is incorporated opposite dG with a half-life of 40 ms, while the incorporation opposite O^6-Me-dG is only slightly slower with a half-life of 60 ms. The incorporation of dTTP opposite O^6-Me-dG is considerably slower with a half-life of 1 s. The incorporation of dCTP opposite O^6-POB-dG is extremely slow with a half-life of >1000 s. With dT modification, both O^2-Me-dT and O^2-POB-dT reacted very slowly. dGTP is the most reactive triphosphate, with $t_{1/2} > 1000\ s^{-1}$. These results are very different from the steady-state kinetics.

We more fully examined these reactions with the six DNA substrates with pol ν in excess. The method is illustrated in Figure 4 in which 15 nM DNA containing O^6-Me-dG and 150 nM pol ν were reacted with various concentrations of dCTP. The time courses (panel A) were fitted to the burst eq (eq 2). Both the burst rates and amplitudes were dependent on the dCTP concentration. Therefore, we fit those parameters to the hyperbolic eq 1 as illustrated in panel B. The results are presented in Table 2, and the k_{pol}/K_d^{dNTP} values are summarized in Figure 5.

The kinetic parameters for the dG template are similar to what we previously observed with a slightly different sequence. In this work, with dT and dG as templates we obtained k_{pol} parameters of 62 and 59 s^{-1} and apparent K_d^{dNTP} values of 6.2 and 24 μM, respectively. These values are similar to a k_{pol} of 100 s^{-1} and a K_d^{dNTP} of 20 μM found previously.[35] Misincorporation occurs with k_{pol} values of 10 to 32 s^{-1} and apparent K_d^{dNTP} values of 47 to 136 μM. As we previously observed, the amplitude of the rapid reaction was also dependent on dNTP concentrations. The A_{max}/[pol] values were similar for all dNTP/template pairings, and ranged from 0.5 to 0.74. The largest differences occurred in the K_A values, which were 5 μM for correct incorporation and 17 to 101 μM for misincorporation.

For O^6-Me-dG, all dNTPs are reactive with the relative preference of dC > dT and dG > dA. The preference for dCTP is not based upon a single dominant parameter but is due to a combination of effects. dCTP has the largest k_{pol}, 39 s^{-1} versus 14 s^{-1} for dTTP. dCTP has the lowest apparent K_d^{dNTP} of 30 μM and dTTP the largest with 140 μM. While all dNTPs have A_{max} values from 0.54 to 0.65, and dCTP has the lowest K_A at 5.8 μM versus 140 μM for dATP.

In spite of similar k_{cat}/K_m values, the other modified nucleotides reacted very slowly in the polymerase in excess experiments. The reduced activities are due to small k_{pol} values. O^6-POB-dG is bypassed slowly, with k_{pol} values 10,000-fold lower than those for O^6-Me-dG. Similarly, the O^2-alkyl-dTs react very slowly with k_{pol} values in the range of 0.001 s^{-1}. The k_{ss} values that were calculated were in the range from 0.005 to 0.05 s^{-1}, similar to the k_{cat} values.

Decreased burst amplitudes associated with replication of DNA damage have generally been associated with the formation of inactive complexes.[35] For example, the A-family T7 DNA polymerase forms are inactive during the insertion of dCTP and dTTP opposite O^6-Me-dG.[38] The decreased burst amplitudes associated with the pol ν bypass of the four adducts studied in this article can potentially be due to this phenomena. We modeled the time courses of the insertions of dCTP opposite O^6-Me-dG and O^6-POB-dG, and dATP opposite O^2-Me-dT and O^2-POB-dT with the seven-step polymerase mechanism. The results shown in Figures S13–S16 demonstrate that the seven-step polymerase mechanism can explain the reduced burst amplitudes. Thus, there is no reason to invoke a more complicated mechanism to explain the results. However, these data do not exclude the possibility of inactive complexes.

DISCUSSION

Pol ν is a low fidelity polymerase because it is very efficient at catalyzing the incorporation of the wrong dNTP.[35] In addition, pol ν produces G/T mispairs at a high frequency, in a sequence-specific manner.[27,39] The current paradigm is that high fidelity polymerases use geometric selection to favor the formation of the Watson–Crick base pairs. During the formation of a mispair, BF was found to exist in an “ajar” structure in which the polymerase was in a state intermediate between the open and closed conformations.[40] This conformation might allow BF to react with the non-Watson–Crick structures in the active site. Pol ν adopts an ajar structure with a Watson–Crick base pair in binding pocket.[41] Therefore, pol ν may naturally exist in a conformation that allows for the rapid formation of mispairs and small damage such as O^6-Me-dG and O^2-Me-dT. It was this property of pol ν, in addition to the similarities between base-pair structures of the G/T mispair and potential O^6-Me-dG and O^2-Me-dT base pairs that led us to test whether pol ν was able to rapidly bypass O^6-alkyl-dG and O^2-alkyl-dT.

Upon the basis of steady-state analysis, the k_{cat}/K_m for the incorporation of dCTP decreased 300-fold for O^6-Me-dG versus dG, values very similar to those found for other enzymes.[10,12–16] However, pol ν differs from other polymerase in the reactivity of dTTP. Typically, methylation of the O^6-position of dG increases the k_{cat}/K_m for dTTP 100-fold.[10,12–16] However, with pol ν, the k_{cat}/K_m for the insertion of dTTP opposite O^6-Me-dG did not increase but decreased 10-fold. The k_{cat}/K_m values for dTTP were similar to those of dATP and dGTP. While high fidelity A-family polymerases select for Watson–Crick geometry, pol ν has less stringent geometrical constraints.

The bypass of various DNA damage with various polymerases have been examined with presteady-state kinetics. The studies show that the reactions are biphasic, with a rapid phase

followed by a slower phase. Kinetic modeling of the data indicates the presence of both active and inactive polymerase/DNA/dNTP complexes.[24,42,43] In the case of T7 pol, an A-family polymerase, and O^6-Me-dG, the rate of the rapid phase is very similar to the rate of correct base pair formation.[14,38] The amplitude of the burst was low, 6–12% of the total enzyme concentration. The kinetic data are consistent with a mechanism in which the pol-DNA-dNTP ternary complex exists in both active and inactive conformations. The burst rate is due to the reaction of the active complex, while the slow phase is either reaction of the inactive complex or conversion of the inactive complex to the active complex.

Pol ν catalyzed incorporation opposite O^6-Me-dG also exhibits biphasic kinetics. However, in contrast to the results observed with T7 pol, the burst amplitude remains the same for the template O^6-Me-dG. The reaction is slightly slower, the k_{pol} for dCTP drops 33%, while the K_d^{dNTP} rises from 6 to 30 μM. Kinetic modeling was undertaken to determine if unreactive pol/DNA/dNTP complexes are necessary to account for the reduced burst amplitudes (Figure S13–S16). However, just as with the undamaged template,[35] a rate limiting step after phosphodiester bond formation can account for the biphasic kinetics. An inactive complex that is off the reaction pathway is not necessary to account for the kinetics. Thus, there is no evidence of active and inactive complexes with pol ν. Whatever the base pair structures in the binding pocket, pol ν rapidly catalyzes phosphodiester bond formation.

Pol ν is able to bypass dA with bulky N^6-adducts such as peptides and oligonucleotides that would be derived from protein and DNA cross-links.[29] However, in an apparent contradiction, pol ν is inefficient at bypassing the smaller N^6-(7,8,9-trihydroxy-7,8,9,10-tetrahydrobenzo[*a*]pyrene)-*d* (N^6-BP-dA).[29] We found that pol ν is very inefficient at bypassing O^6-POB-dG. The k_{pol} for the incorporation opposite O^6-POB-dG is 5-orders of magnitude lower than that opposite O^6-Me-dG. There are no obvious steric clashes in the crystal structure of pol ν[44] that would prevent O^6-POB-dG or N^6-BP-dA from being a substrate. The mechanism underlying the reduced reactivity of moderately sized DNA adducts in the major groove is unknown.

We evaluated the reactivity of pol ν with O^2-Me-dT because O^2-Me-dT can potentially form Watson–Crick-like and wobble structures with dG (Figure 1E and F). In this regard, it has similarities with O^6-Me-dG. However, we found that O^2-Me-dT and O^2-POB-dT are very poor substrates for pol ν. The k_{pol} values are ~50,000-fold lower than that for the incorporation of dATP opposite dT. Thus, while pol ν rapidly forms mispairs and can bypass small damage such as O^6-Me-dG and thymine glycol, the identity of the damage does influence reactivity. A-family polymerases Kf and T7 pol are sensitive to damage on the minor groove side of the DNA.[24,45] This property is conserved with pol ν. Perhaps, as with other A-family polymerases, close contacts with the minor groove of the DNA are involved in providing a high catalytic state.[46,47]

One aim of this work was to evaluate the possibility that pol ν has the in vitro catalytic activity to potentially bypass these adducts in vivo. The catalytic activity of pol ν toward O^6-Me-dG is higher than that reported for any other polymerase.[14,19,38] Therefore, pol ν has the potential to contribute to the bypass of O^6-Me-dG in vivo. With regard to O^6-POB-dG,

O^2-Me-dT, and O^2-POB-dT, the catalytic activity of pol ν is much lower than that for pol η,[13,25] and thus, it is highly unlikely to be involved it the bypass of these adducts.

Supplementary Material

Refer to Web version on PubMed Central for supplementary material.

Acknowledgments

Funding

This project was funded under NIH grant no. ES021762.

The oligodeoxynucleotide synthesis and MS analysis were performed in the Macromolecular Core facility at the PSU College of medicine. The NMR spectra were recorded in the solution NMR core facility. Core Facility services and instruments used in this project were funded, in part, under a grant with the Pennsylvania Department of Health using Tobacco Settlement Funds.

ABBREVIATIONS

BF	*Bacillus stearothermophilus* DNA polymerase I large fragment
Kf(exo-)	Klenow fragment of proofreading deficient *E. coli* DNA polymerase I
NNK	4-(methylnitrosamino)-1-(3-pyridyl)-1-butanone
***O*^{6}-Me-dG**	O^2-methyl-2′-deoxyguano-sine
***O*^{2}-Me-dT**	O^2-methylthymidine
***O*^{6}-POB-dG**	O^6-[4-(3-pyridyl)-4-oxobut-1-yl]-2′-deoxyguanosine
***O*^{2}-POB-dT**	O^2-[4-(3-pyridyl)-4-oxobut-1-yl]thymidine
POB	4-(3-pyridyl)-4-ox-obut-1-yl
pol	polymerase
pol	polymerase

References

1. Cancer Facts and Figures, 2014. American Cancer Society; Atlanta, GA: 2014.
2. Hecht SS. Tobacco smoke carcinogens and lung cancer. J Natl Cancer Inst. 1999; 91:1194–1210. [PubMed: 10413421]
3. Hecht SS. Tobacco carcinogens, their biomarkers and tobacco-induced cancer. Nat Rev Cancer. 2003; 3:733–744. [PubMed: 14570033]
4. IARC. IARC Monographs on the Evaluation of Carcinogenic Risks to Humans. World Health Organization, International Agency for Research on Cancer; Lyon, France: 2004. Tobacco Smoke and Involuntary Smoking; p. 53-119.
5. Hecht SS, Jordan KG, Choi CI, Trushin N. Effects of deuterium substitution on the tumorigenicity of 4-(metlhylnitrosamino)-1-(3-pyridyl)-1-butanone and 4-(methylnitrosa-mino)-1-(3-pyridyl)-1-butanol in A/J mice. Carcinogenesis. 1990; 11:1017–1020. [PubMed: 2347060]

6. Hecht SS, Lin D, Castonguay A, Rivenson A. Effects of alpha-deuterium substitution on the tumorigenicity of 4-(methylnitrosamino)-1-(3-pyridyl)-1-butanone in F344 rats. Carcino-genesis. 1987; 8:291–294.
7. Peterson LA, Hecht SS. O^6 -Methylguanine is a critical determinant of 4-(methylnitrosamino)-1-(3-pyridyl)-1-buta-none tumorigenesis in A/J mouse lung. Cancer Res. 1991; 51:5557–5564. [PubMed: 1913675]
8. Pauly GT, Peterson LA, Moschel RC. Mutagenesis by O^6-[4-oxo-4-(3-pyridyl)butyl]guanine in Escherichia coli and human cells. Chem Res Toxicol. 2002; 15:165–169. [PubMed: 11849042]
9. Weerasooriya S, Jasti VP, Bose A, Spratt TE, Basu AK. Roles of translesion synthesis DNA polymerases in the potent mutagenicity of tobacco-specific nitrosamine-derived O-alkylthymidines in human cells. DNA Repair. 2015; 35:63–70. [PubMed: 26460881]
10. Dosanjh MK, Galeros G, Goodman MF, Singer B. Kinetics of extension of O 6 -methylguanine paired with cytosine or thymine in defined oligonucleotide sequences. Biochemistry. 1991; 30:11595–11599. [PubMed: 1747377]
11. Singh J, Su L, Snow ET. Replication across O6-Methylguanine by Human DNA Polymerase beta in Vitro. J Biol Chem. 1996; 271:28391–28398. [PubMed: 8910463]
12. Snow ET, Foote RS, Mitra S. Base-pairing properties of O 6 -methylguanine in template DNA during in vitro DNA replication. J Biol Chem. 1984; 259:8095–8100. [PubMed: 6376499]
13. Choi JY, Chowdhury G, Zang H, Angel KC, Vu CC, Peterson LA, Guengerich FP. Translesion synthesis across O^6-alkylguanine DNA adducts by recombinant human DNA polymerases. J Biol Chem. 2006; 281:38244–38256. [PubMed: 17050527]
14. Woodside AM, Guengerich FP. Effect of the O^6-substituent on misincorporation kinetics catalyzed by DNA polymerases at O^6-methylguanine and O^6-benzylguanine. Biochemistry. 2002; 41:1027–1038. [PubMed: 11790127]
15. Haracska L, Prakash S, Prakash L. Replication past O(6)-methylguanine by yeast and human DNA polymerase eta. Mol Cell Biol. 2000; 20:8001–8007. [PubMed: 11027270]
16. Spratt TE, Levy DE. Structure of the hydrogen bonding complex of O^6-methylguanine with cytosine and thymine during DNA replication. Nucleic Acids Res. 1997; 25:3354–3361. [PubMed: 9241252]
17. Loveless A. Possible relevance or O-6 alkylation of deoxyguanosine to the mutagenicity and carcinogenecity of nitros-amines and nitrosamides. Nature. 1969; 223:206–207. [PubMed: 5791738]
18. Warren JJ, Forsberg LJ, Beese LS. The structural basis for the mutagenicity of O^6-methyl-guanine lesions. Proc Natl Acad Sci U S A. 2006; 103:19701–19706. [PubMed: 17179038]
19. Washington MT, Johnson RE, Prakash L, Prakash S. Accuracy of lesion bypass by yeast and human DNA polymerase eta. Proc Natl Acad Sci U S A. 2001; 98:8355–8226. [PubMed: 11459975]
20. Zhai Q, Wang P, Cai Q, Wang Y. Syntheses and characterizations of the in vivo replicative bypass and mutagenic properties of the minor-groove O^2-alkylthymidine lesions. Nucleic Acids Res. 2014; 42:10529–10537. [PubMed: 25120272]
21. Jasti VP, Spratt TE, Basu AK. Tobacco-specific nitrosamine-derived O^2-alkylthymidines are potent mutagenic lesions in SOS-induced *Escherichia coli*. Chem Res Toxicol. 2011; 24:1833–1835. [PubMed: 22029400]
22. Andersen N, Wang J, Wang P, Jiang Y, Wang Y. In-vitro replication studies on O^2-methylthymidine and O^4-methyl-thymidine. Chem Res Toxicol. 2012; 25:2523–2531. [PubMed: 23113558]
23. Andersen N, Wang P, Wang Y. Replication across regioisomeric ethylated thymidine lesions by purified DNA polymerases. Chem Res Toxicol. 2013; 26:1730–1738. [PubMed: 24134187]
24. Gowda ASP, Krishnegowda G, Suo Z, Amin S, Spratt TE. Low Fidelity Bypass of O2-(3-Pyridyl)-4-oxobutylth-ymine, the Most Persistent Bulky Adduct Produced by the Tobacco Specific Nitrosamine 4-(Methylnitrosamino)-1-(3-pyridyl)-1-butanone by Model DNA Polymerases. Chem Res Toxicol. 2012; 25:1195–1202. [PubMed: 22533615]
25. Gowda ASP, Spratt TE. DNA Polymerases η and ζ Combine to Bypass O2-[4-(3-Pyridyl)-4-oxobutyl]thymine, a DNA Adduct Formed from Tobacco Carcinogens. Chem Res Toxicol. 2016; 29:303–316. [PubMed: 26868090]

26. Takata, K-i, Shimizu, T., Iwai, S., Wood, RD. Human DNA polymerase N (POLN) Is a low fidelity enzyme capable of error-free bypass of 5S-thymine glycol. J Biol Chem. 2006; 281:23445–23455. [PubMed: 16787914]
27. Arana ME, Takata K-i, Garcia-Diaz M, Wood RD, Kunkel TA. A unique error signature for human DNA polymerase ν. DNA Repair. 2007; 6:213–223. [PubMed: 17118716]
28. Zietlow L, Smith LA, Bessho M, Bessho T. Evidence for the involvement of human DNA polymerase N in the repair of DNA interstrand cross-links. Biochemistry. 2009; 48:11817–11824. [PubMed: 19908865]
29. Yamanaka K, Minko IG, Takata K-i, Kolbanovskiy A, Kozekov ID, Wood RD, Rizzo CJ, Lloyd RS. Novel enzymatic function of DNA polymerase ν in translesion DNA synthesis past major groove DNA–peptide and DNA–DNA cross-links. Chem Res Toxicol. 2010; 23:689–695. [PubMed: 20102227]
30. Johnson SJ, Beese LS. Structures of mismatch replication errors observed in a DNA polymerase. Cell. 2004; 116:803–816. [PubMed: 15035983]
31. Wang W, Hellinga HW, Beese LS. Structural evidence for the rare tautomer hypothesis of spontaneous mutagenesis. Proc Natl Acad Sci U S A. 2011; 108:17644–17648. [PubMed: 22006298]
32. Dunn, DB., Hall, RH. Handbook of Biochemistry and Molecular Biology. Fasman, GD., editor. CRC Press; Boca Raton, FL: 1986. p. 65-215.
33. Krishnegowda G, Sharma AK, Krzeminski J, Gowda ASP, Lin JM, Desai D, Spratt TE, Amin S. Facile syntheses of O^2-[4-(3-pyridyl-4-oxobut-1-yl]thymidine, the major adduct formed by tobacco specific nitrosamine 4-methylnitrosamino-1-(3-pyridyl)-1-butanone (NNK) in vivo, and Its site-specifically adducted oligodeoxynucleotides. Chem Res Toxicol. 2011; 24:960–967. [PubMed: 21524094]
34. Coulter R, Blandino M, Tomlinson JM, Pauly GT, Krajewska M, Moschel RC, Peterson LA, Pegg AE, Spratt TE. Differences in the rate of repair of O6-alkylguanines in different sequence contexts by O6-alkylguanine-DNA alkyltransferase. Chem Res Toxicol. 2007; 20:1966–1971. [PubMed: 17975884]
35. Gowda AS, Moldovan GL, Spratt TE. Human DNA Polymerase nu Catalyzes Correct and Incorrect DNA Synthesis with High Catalytic Efficiency. J Biol Chem. 2015; 290:16292–16303. [PubMed: 25963146]
36. Kuzmic P. DynaFit–a software package for enzymology. Methods Enzymol. 2009; 467:247–280. [PubMed: 19897096]
37. Takata, K-i, Arana, ME., Seki, M., Kunkel, TA., Wood, RD. Evolutionary conservation of residues in vertebrate DNA polymerase N conferring low fidelity and bypass activity. Nucleic Acids Res. 2010; 38:3233–3244. [PubMed: 20144948]
38. Woodside AM, Guengerich FP. Misincorpora-tion and stalling at O^6-methylguanine and O^6-benzylguanine: evidence for inactive polymerase complexes. Biochemistry. 2002; 41:1039–1050. [PubMed: 11790128]
39. Arana ME, Potapova O, Kunkel TA, Joyce CM. Kinetic analysis of the unique error signature of human DNA polymerase nu. Biochemistry. 2011; 50:10126–10135. [PubMed: 22008035]
40. Wu EY, Beese LS. The Structure of a High Fidelity DNA Polymerase Bound to a Mismatched Nucleotide Reveals an “Ajar” Intermediate Conformation in the Nucleotide Selection Mechanism. J Biol Chem. 2011; 286:19758–19767. [PubMed: 21454515]
41. Lee YS, Gregory MT, Yang W. Human Pol ζ purified with accessory subunits is active in translesion DNA synthesis and complements Pol η in cisplatin bypass. Proc Natl Acad Sci U S A. 2014; 111:2954–2959. [PubMed: 24449906]
42. Vyas R, Efthimiopoulos G, Tokarsky EJ, Malik CK, Basu AK, Suo Z. Mechanistic Basis for the Bypass of a Bulky DNA Adduct Catalyzed by a Y-Family DNA Polymerase. J Am Chem Soc. 2015; 137:12131–12142. [PubMed: 26327169]
43. Sherrer SM, Sanman LE, Xia CX, Bolin ER, Malik CK, Efthimiopoulos G, Basu AK, Suo Z. Kinetic Analysis of the Bypass of a Bulky DNA Lesion Catalyzed by Human Y-Family DNA Polymerases. Chem Res Toxicol. 2012; 25:730–740. [PubMed: 22324639]

44. Lee YS, Gao Y, Yang W. How a homolog of high-fidelity replicases conducts mutagenic DNA synthesis. Nat Struct Mol Biol. 2015; 22:298–303. [PubMed: 25775266]

45. Zang H, Harris TM, Guengerich FP. Kinetics of Nucleotide Incorporation Opposite DNA Bulky Guanine N2 Adducts by Processive Bacteriophage T7 DNA Polymerase (Exonuclease-) and HIV-1 Reverse Transcriptase. J Biol Chem. 2005; 280:1165–1178. [PubMed: 15533946]

46. Meyer AS, Blandino M, Spratt TE. E. coli DNA polymerase I (Klenow fragment) uses a hydrogen bonding fork from Arg668 to the primer terminus and incoming deoxynucleotide triphosphate to catalyze DNA replication. J Biol Chem. 2004; 279:33043–33046. [PubMed: 15210707]

47. McCain MD, Meyer AS, Glekas A, Spratt TE. Fidelity of mispair formation and mispair extension is dependent on the interaction between the minor groove of the primer terminus and Arg668 of DNA Polymerase I of E. coli. Biochemistry. 2005; 44:5647–5659. [PubMed: 15823023]

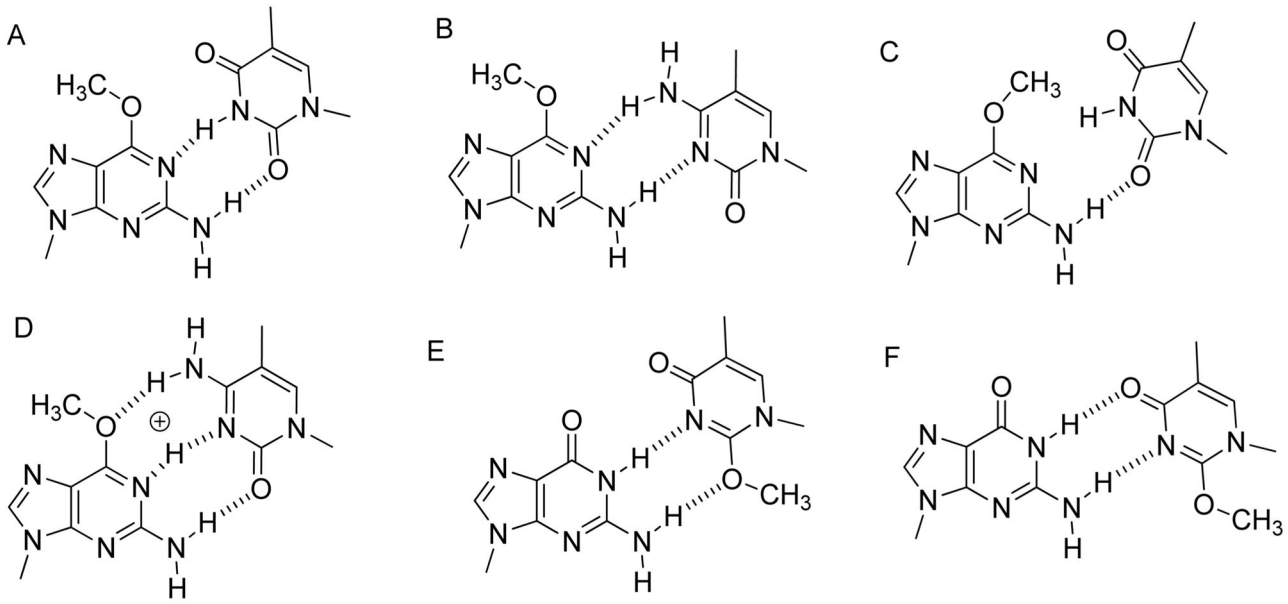

Figure 1.
Potential base pair structures.

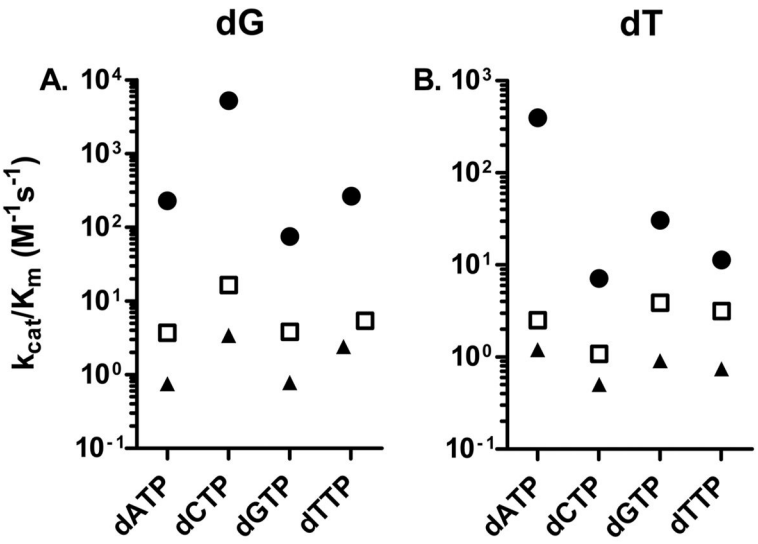

Figure 2.

Relative k_{cat}/K_m values for the single nucleotide incorporation opposite (A) dG(closed circle), O^6-Me-dG (open square), and O^6-POB-dG (closed triangle), and (B) dT (closed circle), O^2-Me-dT (open square), and O^2-POB-dT (closed triangle).

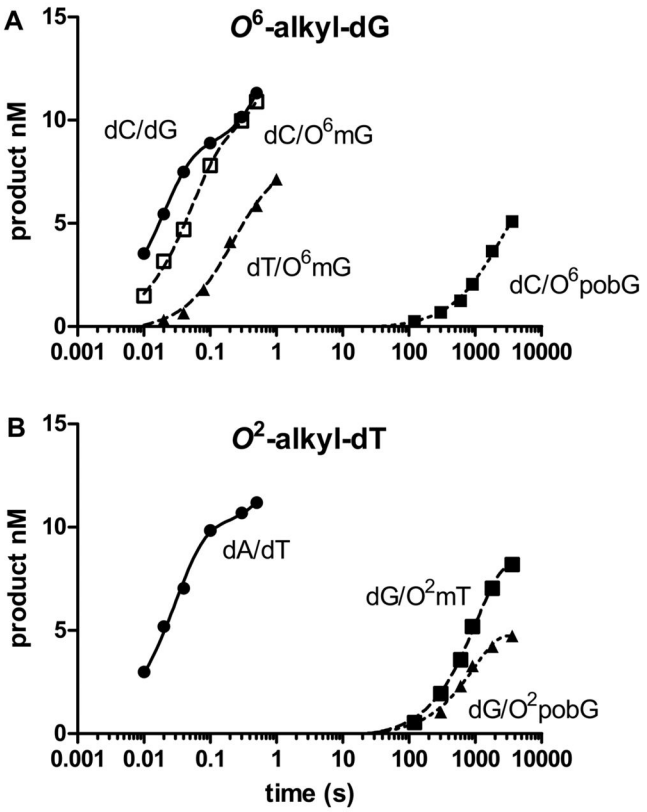

Figure 3.

Incorporation of single dNTPs opposite templates containing (A) dG and (dT) and analogues. The concentration of the DNA was 15 nM, the pol 150 nM, and the dNTP was 50 μM.

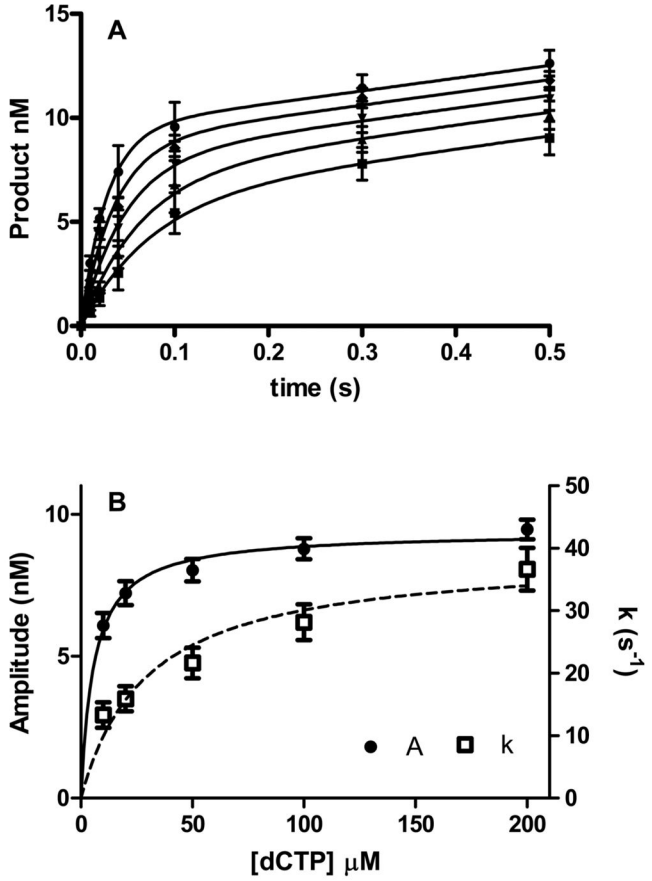

Figure 4.

Analysis of the time course data. (A) Incorporation of pol ν (150 nM) catalyzed dCTP (10, square; 20, triangle; 50, upside down triangle; 100, diamond; and 200, circle μM) incorporation opposite DNA containing O^6-Me-dG (15 nM). The lines are the best fit to equation 1. The error bars represent the standard deviation of three determinations. (B) Plot of amplitude (A) and burst rate constant (k) versus dCTP concentration. The lines are the best fit to eq 2, and the error bars are the standard errors.

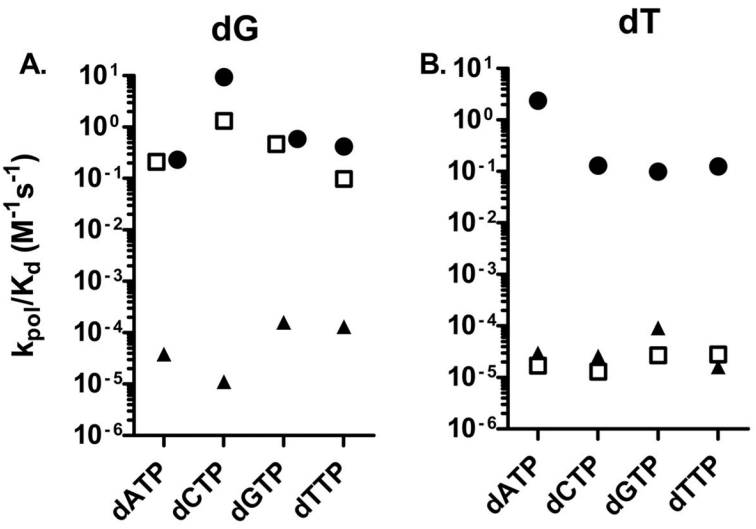

Figure 5.

Relative k_{pol}/K_d values for the single nucleotide incorporation opposite (A) dG(closed circle), O^6-Me-dG (open square), O^6-POB-dG (closed triangle), and (B) dT (closed circle), O^2-Me-dT (open square), and O^2-POB-dT (closed triangle).

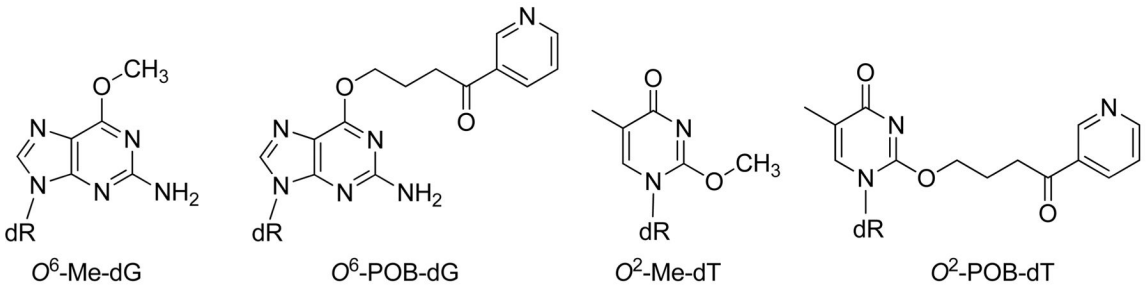

Chart 1.

P15-	5′- G C A C C G C A G A C G C A G -3′
T24(G)	3′- C G T G G C G T C T G C G T C **X** T C A G C G T C -5'
T24(T)	3′- C G T G G C G T C T G C G T C **Y** G C A G C G T C -5'

Chart 2.
Oligodeoxynucleotide sequences

Table 1

Steady State Kinetic Parameters for the Pol ν Catalyzed Insertion Opposite O^6-Alkyl-dG and O^2-Alkyl-dT[a]

dNTP	template	k_{cat} ($s^{-1} \times 10^3$)	K_m (μM)	k_{cat}/K_m ($M^{-1} s^{-1}$)	f_{inc}
dATP	dG	12.5 ± 0.5	230 ± 22	55 ± 3	0.010
dCTP	dG	30.9 ± 0.7	5.9 ± 0.5	5220 ± 310	1
dGTP	dG	5.4 ± 0.1	76 ± 6	75 ± 5	0.014
dTTP	dG	13.7 ± 0.6	52 ± 7	264 ± 25	0.051
dATP	O^6-Me-dG	3.05 ± 0.23	820 ± 110	3.7 ± 0.2	0.23
dCTP	O^6-Me-dG	6.61 ± 0.52	400 ± 56	16.5 ± 1.1	1
dGTP	O^6-Me-dG	3.68 ± 0.38	970 ± 160	3.8 ± 0.3	0.23
dTTP	O^6-Me-dG	4.62 ± 0.55	860 ± 180	5.4 ± 0.5	0.33
dATP	O^6-POB-dG	0.48 ± 0.05	636 ± 111	0.75 ± 0.07	0.22
dCTP	O^6-POB-dG	1.18 ± 0.08	350 ± 57	3.4 ± 0.3	1
dGTP	O^6-POB-dG	0.67 ± 0.07	860 ± 150	0.78 ± 0.07	0.23
dTTP	O^6-POB-dG	0.78 ± 0.04	331 ± 46	2.4 ± 0.2	0.70
dATP	dT	24.1 ± 1.5	61 ± 7	396 ± 24	1
dCTP	dT	1.07 ± 0.02	150 ± 10	7.15 ± 0.35	0.018
dGTP	dT	2.26 ± 0.04	74 ± 4	30.5 ± 1.5	0.077
dTTP	dT	1.18 ± 0.03	104 ± 0 10	11.3 ± 0.9	0.029
dATP	O^2-Me-dT	1.10 ± 0.05	438 ± 43	2.51 ± 0.14	1
dCTP	O^2-Me-dT	0.71 ± 0.05	657 ± 95	1.08 ± 0.08	0.43
dGTP	O^2-Me-dT	1.48 ± 0.05	381 ± 28	3.89 ± 0.17	1.55
dTTP	O^2-Me-dT	1.23 ± 0.04	386 ± 28	3.19 ± 0.14	1.27
dATP	O^2-POB-dT	0.43 ± 0.02	358 ± 34	1.20 ± 0.08	1
dCTP	O^2-POB-dT	0.55 ± 0.04	1100 ± 150	0.50 ± 0.03	0.42
dGTP	O^2-POB-dT	0.553 ± 0.027	605 ± 69	0.91 ± 0.06	0.76
dTTP	O^2-POB-dT	0.49 ± 0.02	660 ± 70	0.74 ± 0.05	0.6261

[a]The kinetic parameters were obtained with 1 nM pol ν and 20 nM DNA. The error is the standard error with three experiments.

Table 2

Kinetic Parameters for the dNTP Dependence of the Pol ν Catalyzed Insertion Opposite O^2-Alkyl-dT

		amplitude		burst rate constant		
		A^{max}/[pol]	$K_A(\mu M)$	$k_{pol}(s^{-1})$	$K_d^{dNTP}(\mu M)$	k_{ss}/[pol] s^{-1}
dATP	dG	0.49 ± 0.01	101 ± 6	32 ± 4	136 ± 58	0.020 ± 0.002
dCTP	dG	0.65 ± 0.02	5.3 ± 1.1	59 ± 2	6.2 ± 1.1	0.038 ± 0.003
dGTP	dG	0.55 ± 0.01	58 ± 7	28 ± 2	47 ± 15	0.020 ± 0.003
dTTP	dG	0.57 ± 0.02	92 ± 12	25 ± 3	60 ± 28	0.017 ± 0.002
dATP	O^6-Me-dG	0.54 ± 0.02	106 ± 12	20 ± 3	93 ± 54	0.011 ± 0.003
dCTP	O^6-Me-dG	0.62 ± 0.02	5.8 ± 0.9	39 ± 4	30 ± 11	0.041 ± 0.01
dGTP	O^6-Me-dG	0.58 ± 0.02	63 ± 9	19 ± 1	40 ± 16	0.021 ± 0.002
dTTP	O^6-Me-dG	0.62 ± 0.0	38 ± 5	14 ± 2	140 ± 50	0.011 ± 0.003
dATP	O^6-POB-dG	0.34 ± 0.02	88 ± 22	0.0014 ± 0.0001	38 ± 7	nd
dCTP	O^6-POB-dG	0.73 ± 0.04	47 ± 11	0.0015 ± 0.0001	146 ± 42	nd
dGTP	O^6-POB-dG	0.37 ± 0.01	240 ± 31	0.0013 ± 0.0002		nd
dTTP	O^6-POB-dG	0.63 ± 0.03	120 ± 18	0.00085 ± 0.00005		nd
dATP	dT	0.74 ± 0.04	5.1 ± 1.8	62 ± 5	26 ± 7	0.027 ± 0.004
dCTP	dT	0.51 ± 0.02	42 ± 9	13 ± 1	100 ± 21	0.008 ± 0.002
dGTP	dT	0.69 ± 0.01	17 ± 2	10 ± 1	101 ± 41	0.007 ± 0.003
dTTP	dT	0.54 ± 0.02	27 ± 6	15 ± 1	118 ± 27	0.012 ± 0.002
dATP	O^2-Me-dT	0.55 ± 0.02	39 ± 7 < 50	0.00150 ± 0.00014	95 ± 32	nd
dCTP	O^2-Me-dT	0.35 ± 0.01	16 ± 5 < 50	0.00113 ± 0.00002	84 ± 7	nd
dGTP	O^2-Me-dT	0.83 ± 0.02	24 ± 3 < 50	0.00212 ± 0.00016	78 ± 22	nd
dTTP	O^2-Me-dT	0.72 ± 0.02	22 ± 4 < 50	0.00238 ± 0.00009	88 ± 12	nd
dATP	O^2-POB-dT	0.37 ± 0.05	78 ± 9	0.00150 ± 0.00014	50 ± 22	nd
dCTP	O^2-POB-dT	0.16 ± 0.01	42 ± 11	0.00117 ± 0.00002	45 ± 4	nd
dGTP	O^2-POB-dT	0.44 ± 0.02	19 ± 4	0.00122 ± 0.00006	13 ± 6	nd
dTTP	O^2-POB-dT	0.21 ± 0.01	46 ± 9	0.00115 ± 0.00002	72 ± 4	nd